Available online at www.sciencedirect.com
ScienceDirect
Trans. Nonferrous Met. Soc. China 27(2017) 272−281
Transactions of Nonferrous Metals Society of China
www.tnmsc.cn

Effect of combinative addition of Ti and Sr on modification of AA4043 welding wire and mechanical properties of AA6082 welded by TIG welding

Bo WANG[1], Song-bai XUE[1], Chao-li MA[1], Yi-long HAN[1], Zhong-qiang LIN[2]

1. College of Materials Science and Technology, Nanjing University of Aeronautics and Astronautics, Nanjing 210016, China;
2. Zhejiang Yuguang Aluminum Material Co., Ltd., Jinhua 321200, China

Received 8 January 2016; accepted 31 August 2016

Abstract: To improve the mechanical properties of AA6082 weld welded by tungsten inert gas welding using AA4043 welding wire, the effect of addition of Ti and/or Sr on continuous cast and rolled AA4043 welding wire was investigated. Experimental results indicated that Ti and Sr are excellent modifiers, which improve the microstructure of the AA4043 welding wire and enhance the mechanical properties of the AA6082 weld. It was found that the combinative addition of Ti and Sr can effectively modify both the α(Al) dendrites and eutectic Si phases compared with individual addition of Ti or Sr. In addition, Ti and/or Sr also changed the microstructure of the AA6082 weld. The tensile strength of the AA6082 weld reached the maximum value when 0.08% Ti and 0.025% Sr were added simultaneously. These results indicate that the combinative addition of Ti and Sr can be an effective composite modifier.

Key words: AA4043 welding wire; titanium; strontium; modification; gas tungsten arc welding; microstructure; mechanical properties

1 Introduction

6000 series aluminum alloys are used extensively for rocket shell, cryogenic tanks, engine castings and other medium strength structures [1]. Therefore, welding of these alloys by different welding methods [2−6] including tungsten inert gas (TIG) welding is considered one of the most important issues in these industries. AHMAD and BAKAR [7] and VERMA et al [8] suggested that AA4043 welding wire is more appropriate for welding of 6000 aluminum alloys, for the alloys of the 6000 series alloys are more sensitive to hot cracking than the alloys of the 5000 series, while AA4043 welding wire is a silicon-based alloy that is often used to take advantage of the elements capability of promoting fluidity in aluminum and is less sensitive to weld cracking. However, it is difficult to obtain a good 6000 series alloy welded joint with good comprehensive mechanical properties using unmodified AA4043 welding wires, because of the large acicular eutectic Si phases and coarse grains that exist in the microstructure of AA4043 welding wires [9,10].

Modification of Al−Si alloys plays a vital role in improving their mechanical properties (ductility and toughness) and various modifiers have been investigated for use in Al−Si castings [11−15]. Rare earth (RE) elements have exhibited certain potency of grain refinement of Al−Si casting alloys. Nevertheless, recent studies have found that excess RE elements (>0.3%) would chemically react with alloying elements, producing needle-like intermetallics which are harmful to mechanical properties of Al−Si alloys [16]. TSAI et al [14] indicated that the modification efficiency in microstructures and mechanical properties of A356 alloy with 1.0% La are similar to those modified by the commercial modifier, 0.012% Sr. These indicate that Sr has greater advantages than rare earth element for modification of Al−Si alloys.

Industrial refiners, such as Al−5Ti−1B, Al−3Ti−1B master alloys, have exerted desirable refinement for wrought aluminum alloys; however, BIROL [17] has

Foundation item: Project (2015A12225) supported by the Key Technical Innovation Project Foundation of Jinhua City, China; Project supported by the Priority Academic Program Development (PAPD) of Jiangsu Higher Education Institutions, China
Corresponding author: Song-bai XUE; Tel: +86-25-84896070; E-mail: xuesb@nuaa.edu.cn
DOI: 10.1016/S1003-6326(17)60031-1

discovered that Al−5Ti−1B master alloy cannot exhibit so remarkable refinement in Al−Si casting alloys. A mutual poisoning effect between B and Sr elements in the Sr-modified Al−Si casting alloys revealed by some researchers [18] limits the practices of binary Al−B or ternary Al−Ti−B master alloy for modification of Sr-containing Al−Si casting alloys.

In order to achieve a better modification of Al−Si alloys and avoid the refinement deterioration of Ti−B for Al−Si casting alloys and mutual poisoning effect between Sr and B, the effect of combinative addition of Ti and Sr without element B which has been rarely reported is worthy of studying. Therefore, in the current work, the microstructure and mechanical properties of the Sr−Ti modified AA4043 welding wire alloy prepared by continuous casting and rolling process (CCRP) and resulting weld welded by TIG welding have been analyzed. Furthermore, the oxidation of Sr during smelting is yet another problem, which should be considered as statistics to indicate that, if the holding time after Sr addition to the high temperature melt exceeds 10 h, elemental Sr cannot be detected in the samples by analysis.

2 Experimental

The compositions of the base material, unmodified AA4043 and modified AA4043 used in this work are listed in Table 1. Preparation of the AA4043 metals was conducted in a homemade flame furnace at 700−760 °C. Ti was added in the form of Al−5Ti master alloy at about 700−750 °C while Sr was added using an Al−10Sr master alloy at 720−730 °C. After refining and degassing, trapezoidal welding wire alloy ingots at temperature of about 400 °C were produced using a continuous casting method and were subsequently heated and hot-rolled to aluminum rods with the diameter 9.5 mm (as illustrated in Fig. 1). The procedures used to prepare the 3.2 mm diameter welding wires included, annealing−drawing−annealing−shaving−cleaning. The base metal was wrought aluminum alloy 6082-T6 plates with dimensions of 12 mm × 175 mm × 350 mm intended for butt welding. Prior to welding, the base material coupons were wire-brushed and degreased with acetone. The welding parameters of different weld passes are given in Table 2. Argon with a purity of 99.99% was used as the shielding gas.

Table 1 Chemical compositions of base metal and welding wires (mass fraction, %)

Material	Si	Fe	Cu	Mn	Mg	Ti	Sr	Al
AA6082	0.96	0.24	0.05	0.56	0.81	0.024	−	Bal.
Welding wire 1	5.0	0.15	−	−	−	0	0	Bal.
Welding wire 2	5.0	0.15	−	−	−	0.08	0	Bal.
Welding wire 3	5.0	0.15	−	−	−	0.15	0	Bal.
Welding wire 4	5.0	0.15	−	−	−	0	0.012	Bal.
Welding wire 5	5.0	0.15	−	−	−	0	0.025	Bal.
Welding wire 6	5.0	0.15	−	−	−	0.08	0.012	Bal.
Welding wire 7	5.0	0.15	−	−	−	0.08	0.025	Bal.

Table 2 Welding parameters

Weld pass	Current polarity	Arc voltage/ V	Arc current/ A	Ar shielding gas/ ($L\cdot min^{-1}$)	Travel speed/ ($cm\cdot min^{-1}$)
1	AC	20	280	11	8−12
2	AC	21−22	285	11	8−12
3	AC	21−22	285	11	8−12
4 (Back)	AC	21−22	285	11	8−12

The residual amounts of Ti or Sr found in the welding wire that was melted with increasing increments of holding time was analyzed using a SPECTRO® MAXx04D spectrometer. The microstructures of the specimens from the center of the trapezoidal welding

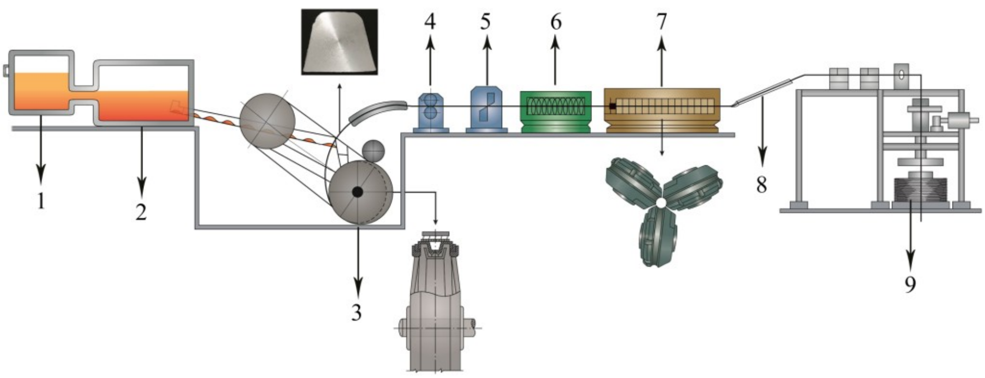

Fig. 1 Schematic illustration of AA4043 rods (9.5 mm in diameter) production: 1—Smelting furnace; 2—Holding furnace; 3—Mould for continuous casting; 4—Conveyer roller; 5—Hydraulic cutter; 6—Medium frequency induction heating device; 7—Y-type rolling mill groups; 8—Laminar flow cooling device; 9—Winder reel

wire alloy ingots and the butt-welded joints were characterized using a TV−400D optical microscopy and a ZEISS ΣIGMA field-emission scanning electron microscope coupled to an energy dispersion X-ray (FE-SEM/EDX). The Vickers hardness measurement was conducted on the base metal and the weld metal using an HXS−1000A microhardness tester under a load of 0.98 N for 15 s. Tensile specimens were prepared from the 9.5 mm aluminum hot-rolled rods and from the welded coupons and the tensile tests were performed on a WAW−300B testing machine.

3 Results and discussion

3.1 Oxidation and loss of Ti (or Sr) from AA4043 melt during holding

Both 0.02% Ti and 0.02% Sr were added to the AA4043 melt separately and the remaining content of Ti or Sr in the alloy melt as function of the holding time is shown in Fig. 2. As shown in Fig. 2, with the holding time increasing, the Sr content in the alloy progressively decreased and the efficiency of the modification resulting from the content of the modifier became weaker (Figs. 2(a)−(c)). When the Sr content was reduced to the critical value of 0.005% or less, there was no effect on the microstructure of the AA4043 alloy, i.e., the modification by the Sr appeared to be time-limited. However, this phenomenon does not appear to be the case with the addition of Ti. As shown in Fig. 2, when Sr was added to the alloy, the holding time of the AA4043 melt should be controlled to within 6 h. Moreover, the optimum content of Sr for casting was 0.005%−0.02%; Sr contents below this range had no effects on the welding wire alloy ingots. Contents of Sr above this range too much caused a dramatic increase of hydrogen absorption by the alloy (Fig. 3).

In the alloy melt, oxidation and loss of Sr can be explained through the use of the Pilling−Bedworth (P−B) ratios (R) [19]. This ratio compares the relative molecular mass and densities of the metal and its respective oxide and is represented by

$$R=\frac{A_{\mathrm{O}}\rho_{\mathrm{M}}}{nA_{\mathrm{M}}\rho_{\mathrm{M}}} \tag{1}$$

where A is the relative molecular mass, ρ is the density, n is the number of atoms of metal per one molecule of the oxide, and the subscripts O and M represents the oxide and metal, respectively. P−B ratios of some metals are listed in Table 3. As can be seen from Table 3, the P−B ratio of Sr is less than unity (even smaller than that of Mg), the molten metal oxide has less volume per molecule than the parent material and therefore cannot fully cover the metal upon oxidation. Figure 4 depicts the formation of oxides according to the P−B ratios of Sr and Ti. From Fig. 4 it can be concluded that Sr is easily oxidized in the high temperature melt if an inert

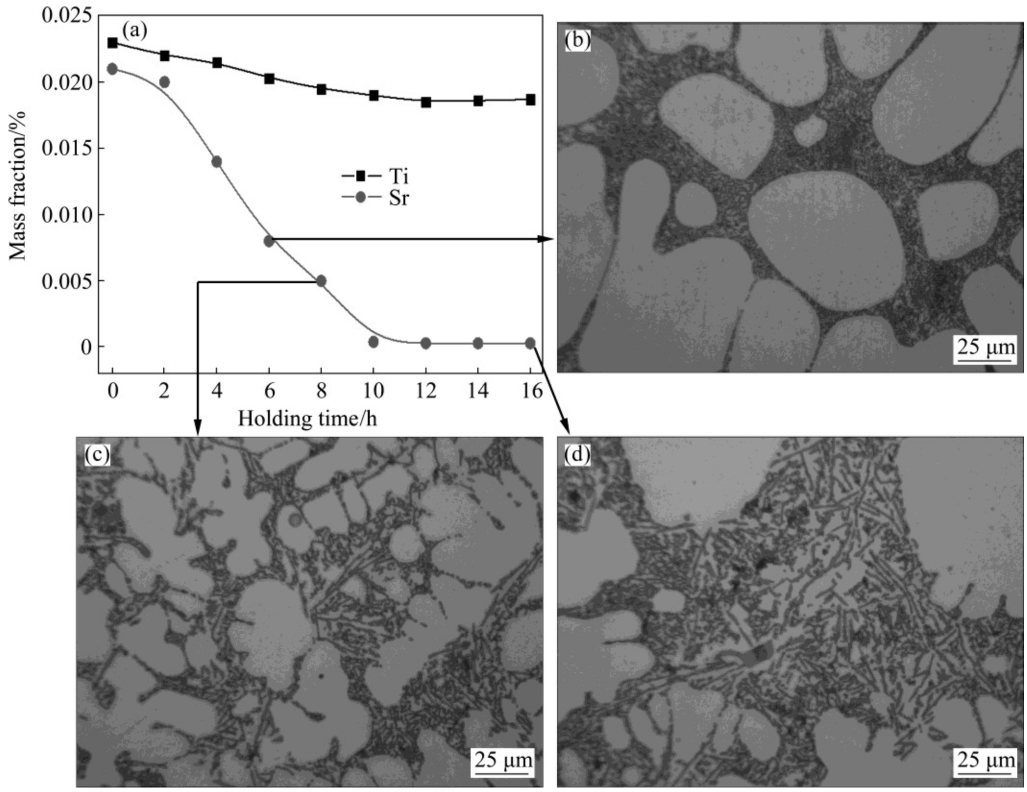

Fig. 2 Remaining content of Ti (or Sr) in aluminum melt with holding time (a) and microstructures (b−d) of Al−5Si−xSr welding wires cooled directly by water: (b) x=0.008; (c) x=0.005; (d) x=0

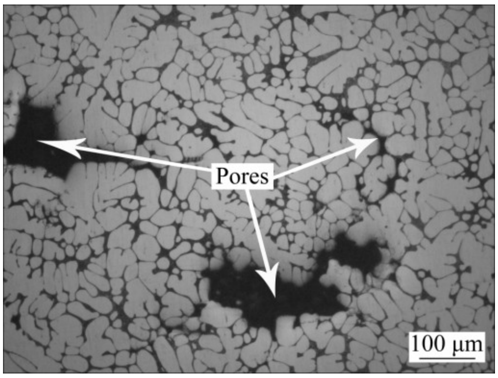

Fig. 3 Porosity in Al−5Si−0.04Sr casting microstructures

Table 3 P−B ratios of some metals

Metal	P−B ratio	Protective
Al	1.28	Yes
Cu	1.7	Yes
Mg	0.84	No
Mn	2.07	Yes
Si	2.04	Yes
Na	0.32	No
Ti	1.73	Yes
Sr	0.69	No

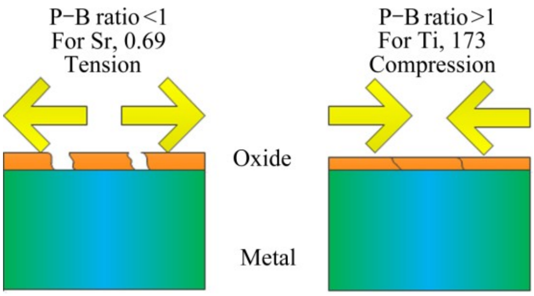

Fig. 4 Oxide stresses according to P−B ratios

atmosphere is not present and plays a role in accelerating the oxidation of Al−Si alloys. Furthermore, SHABESTARI et al [20] studied the effect of Sr-modification on hydrogen content of commercial 319 aluminum alloy melts by using HYSCAN instrument at 685 °C and 735 °C and declared that SrO in the surface oxide layer should account for the higher hydrogen content of uncleaned melts in Sr-modified alloys compared to the unmodified alloys. LIU et al [21] found that pores observed in Sr-modified alloys are frequently associated with Sr oxides (films or particles). Therefore, in order to make the best of the modification of elemental Sr, the holding time of melting and upper limit of the additive amount should be controlled within 6 h and 0.02%, respectively.

3.2 Effect of Ti or Sr modification on microstructure of AA4043 welding wire alloy

3.2.1 Evolution of microstructures of Ti modified AA4043 welding wire alloy

Figure 5 shows the microstructure of the AA4043 alloys with different Ti contents. As shown in Fig. 5(a), coarse columnar α(Al) dendrites can be seen in the AA4043 alloy starting material (no alloying Ti). The size of the coarse dendrites was altered significantly and refined equiaxed α(Al) grains were obtained with the addition of 0.08% Ti. This result is evident from inspection of Fig. 5(b). However, with a further increase in Ti content (up to 0.15% Ti), the grain morphology remained equiaxed but the grain size increased.

Focusing on the eutectic Si phases in AA4043 alloys with different Ti contents, one can find that the efficacy of the modification of Ti on the morphology of eutectic Si phases is extremely low. To be specific, as shown in Fig. 5(d), the lamellar eutectic Si particles or needle-like eutectic Si phases precipitated unevenly among α(Al) dendrites in the unmodified AA4043 alloy. The lamellar or needle-like eutectic Si phases were considered to be very brittle and their existence in the structure severely fragmented the aluminum matrix, further reducing the strength and ductility of the AA4043 alloy. By adding 0.08% Ti, the coarse lamellar eutectic Si particles disappeared and the aspect ratio of needle-like structure was slightly reduced. However, further Ti addition of up to 0.15% resulted in the aggregation of the eutectic Si phases. Evidently, addition of Ti element is incapable of modifying the needle-like structures of eutectic Si phases, which is consistent with the comparatively metallographic analysis presented by ZEREN and KARAKULAK [22].

3.2.2 Evolution of microstructures of Sr or Sr−Ti modified AA4043 welding wire alloy

Figure 6 shows the metallographic images of the AA4043 welding wire metal ingots with different Sr and Ti contents. As shown in Figs. 6(a) and (b), as the content of Sr in the Al−5Si−xSr (x=0.012, 0.025) alloy was increased, the size of the α(Al) dendrites decreased slightly. Compared with Al−5Si−xSr (x=0.012, 0.025) alloy, the α(Al) grains of Al−5Si−0.08Ti alloy were further refined. When 0.08% Ti was added into the Al−5Si−xSr (x=0.012, 0.025) welding wire metal ingots, the size of the α(Al) dendrites decreased obviously.

Figure 7 displays the SEM morphologies of the eutectic Si phases of the Al−5Si−0.08Ti welding wire alloys with varied Sr additions. The dark grey area in Fig. 7 represents α(Al) dendrites (identified by EDX analysis result of Point *A* in Table 4), light grey area represents eutectic Si phases (Point *B* and Area *D* in Table 4) and the acicular white phase represents the Fe-bearing intermetallic compound (IMC) (Point *C* in Table 4), which is confirmed to be β-Fe IMC [23]. As shown in Fig. 7, as the content of Sr in the Al−5Si−0.08Ti alloy was increased, the eutectic Si phases transformed from coarse needle-like structures

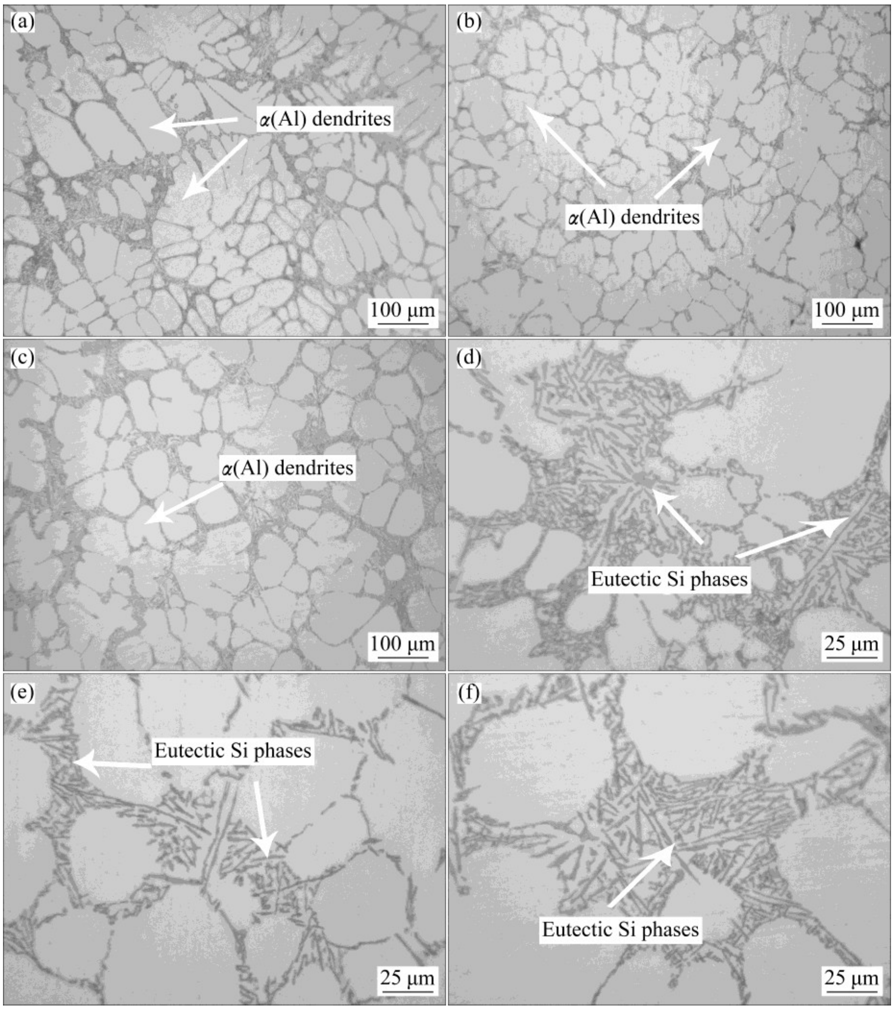

Fig. 5 Microstructures of Al−5Si−xTi welding wire metal ingots: (a) x=0; (b) x=0.08; (c) x=0.15; (d) x=0 at high magnification; (e) x=0.08 at high magnification; (f) x=0.15 at high magnification

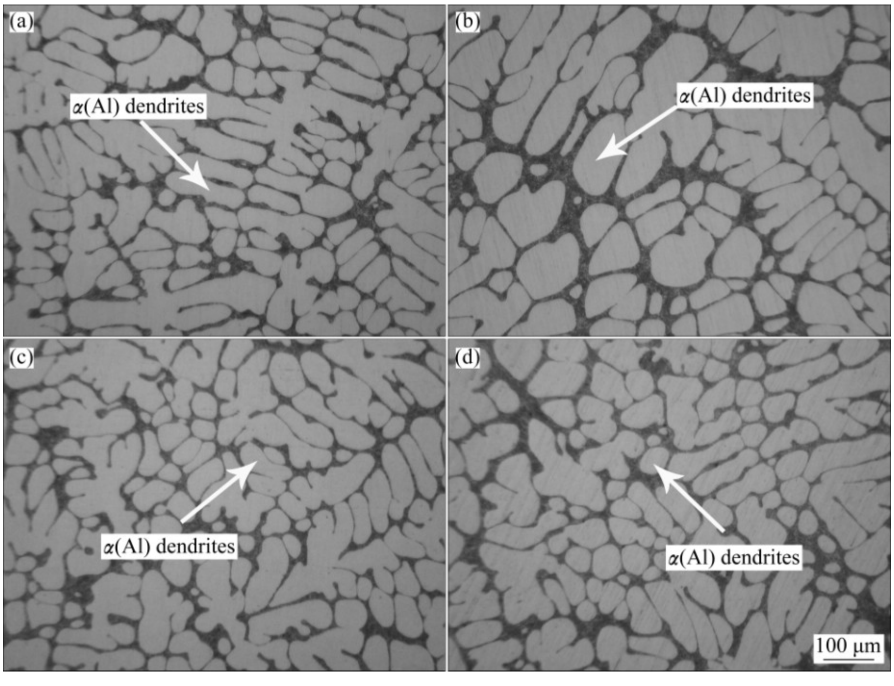

Fig. 6 Microstructures of AA4043 welding wire metal ingots with different contents of Sr and/or Ti: (a) 0.012% Sr+0 Ti; (b) 0.025% Sr + 0 Ti; (c) 0.012% Sr + 0.08% Ti; (d) 0.025% Sr + 0.08% Ti

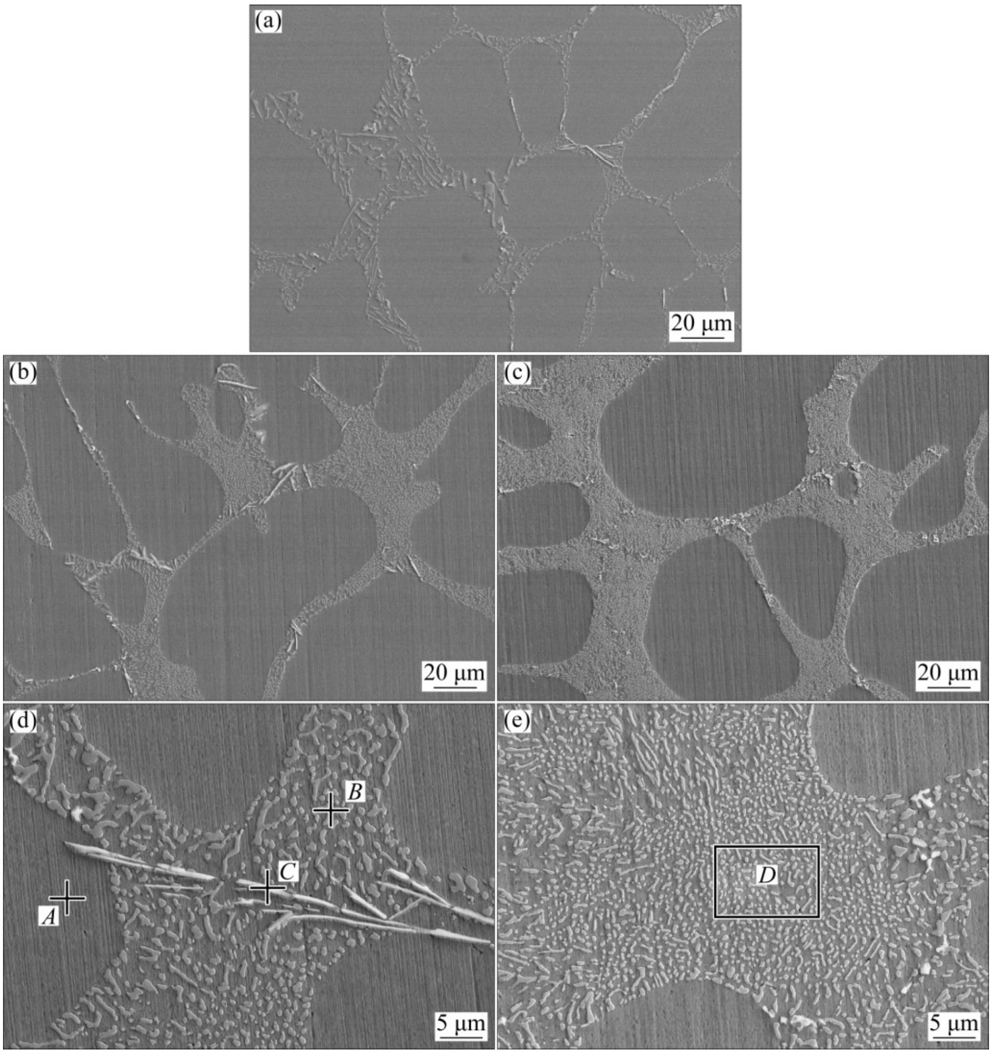

Fig. 7 SEM images of Al−5Si−0.08Ti−xSr welding wire metal ingots: (a) x=0; (b) x=0.012; (c) x=0.025; (d) x=0.012 at high magnification; (e) x=0.025 at high magnification

(Fig. 7(a)) to fine fibrous-like structures (Figs. 7(b) and (c)) that were uniformly distributed in the boundaries of the α(Al) matrix. By comparing Figs. 7(d) and (e), it can be seen that the size and the aspect ratio of the eutectic Si phases were further reduced and fully modified eutectic Si phases with fine particle shapes were obtained with increasing the amount of Sr to 0.025%. Besides, the morphology of β-Fe IMC was also modified from acicular structure to short rod-like structure, which can cause the improvement in mechanical properties of alloy, in particular, the ductility and toughness [23].

Thus, with regard to the improvement of the morphology of the eutectic Si phase and β-Fe IMC, the greater the amount of Sr added to the alloy, the better the properties of the resulting AA4043 alloy. However, there is a limit to the amount of Sr that can be added, beyond which the morphology of the microstructure will be negatively impacted. Figure 8(a) shows the SEM images of Al−5Si−1Sr welding wire alloys, β-Fe IMC again showed an acicular-like morphology (Figs. 8(a) and (d)); elemental Sr chemically reacted with other elements, producing very long needle-like white IMC (Position F in Fig. 8(a)) which is harmful to mechanical properties of AA4043 alloys. The EDX results indicate the composition of this Sr bearing IMC (Point F) to be Al−27.43Si−43.62Sr, which may be the Al_2Si_2Sr phase. In addition, it has been reported that Sr modification of the alloy was the main reason for the increase in porosity in the hypoeutectic Al−Si alloy [20,21].

By comparing Figs. 5(e) and 7(d), it can be seen that Sr modification resulted in a very significant decrease in the aspect ratio of the eutectic Si phases in the AA4043 alloy. Alloys modified with Ti under the same conditions, were not so affected, which indicates that the efficacy of Sr modification of AA4043 welding wire metal is relatively higher than that of Ti addition. However, addition of 0.08% Ti into the Al−5Si−xSr (x=0.012, 0.025) can significantly reduce the size of

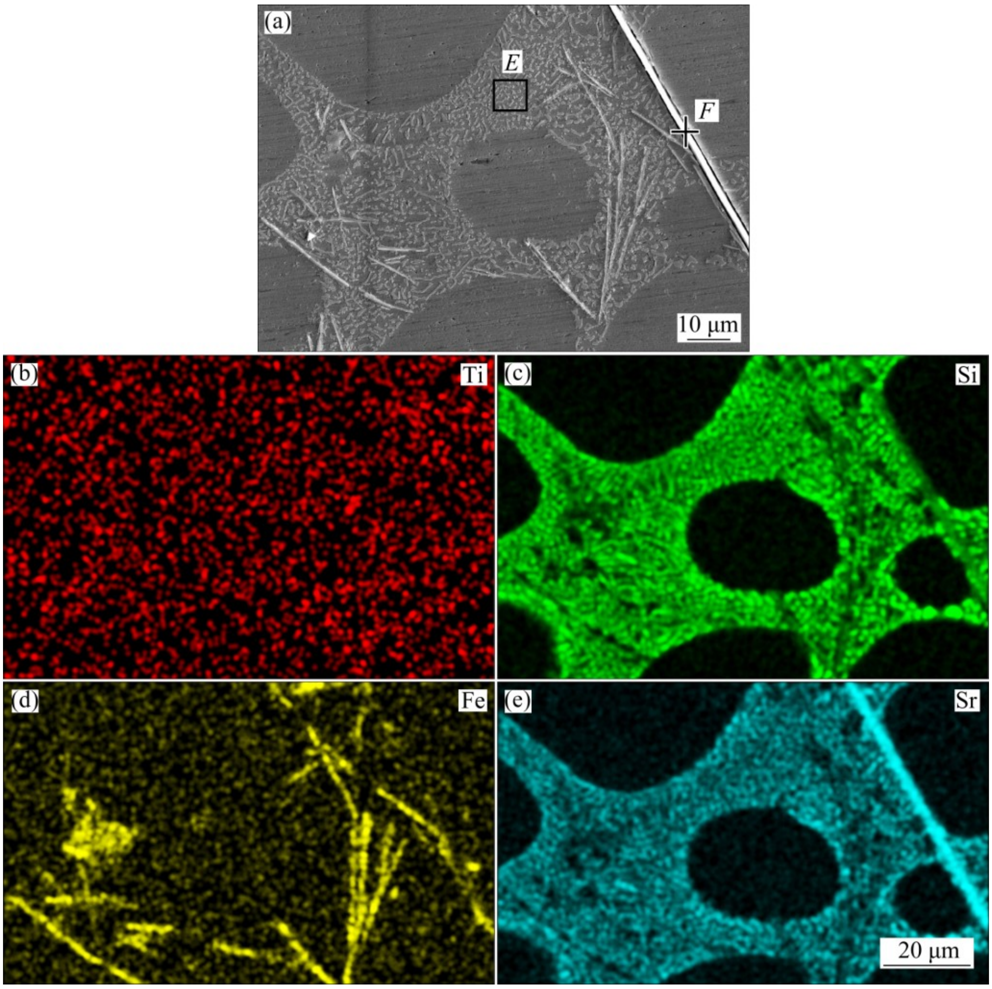

Fig. 8 SEM image of Al−5Si−1Sr welding wire metal ingot and EDX analysis results of element distribution: (a) Al−5Si−1Sr welding wire metal; (b) Ti; (c) Si; (d) Fe; (e) Sr

Table 4 EDX analysis results of points and areas indicated in Figs. 7(d) and (e) and Fig. 8(a) (mass fraction, %)

Point (or Area)	Al	Si	Fe	Sr
A	98.47	1.53	−	−
B	70.74	29.26	−	−
C	59.56	14.83	25.62	−
D (Area)	81.13	18.87	−	−
E (Area)	80.27	18.82	−	0.91
F	28.95	27.43	−	43.62

α(Al) dendrites. Generally speaking, the addition of Ti and Sr can be mutually complemented in modifying the microstructure of AA4043 alloy.

3.2.3 Variation in modification mechanisms between Ti and Sr

Under conventional casting conditions, the eutectic silicon phase, with the characteristic of small flat growth, grows rapidly along the ⟨112⟩ direction into lamellar or coarse acicular eutectic Si crystals. The effect of Ti addition on the primary α(Al) dendrites (Figs. 5 and 6) is mainly described as nucleation modification, where $TiAl_3$ particles [22] from the peritectic reaction of the Al melt and Ti are an effective heterogeneous substrate for formation of α(Al) dendrites. This increases the nucleation rate and hence leads to a transition of the α(Al) phase from a columnar to a fine equiaxed phase.

The effect of Sr modification on the eutectic Si phases of the AA4043 welding wire alloy was superior to that of Ti, as shown in Figs. 5−7. There are two schools of thought in explaining the mechanism of modification of the eutectic Si phases by Sr addition: the poisoning of the twin plane re-entrant edge (TPRE) in the growth of the eutectic Si phase by Sr atoms [24], and the another promotes the idea of Sr playing a more complicated role in interfering with the nucleation of the various secondary phases during solidification while finally evolving as the AlSiSr IMC along with the eutectic Si phases during solidification. The latter school of thought was substantiated with experimental evidences by MANICKARAJ et al [25] using the nano-diffraction technique with a high energy synchrotron beam source coupled with X-ray fluorescence imaging system and they confirmed that elemental Sr does not exist in the solidified Al−Si alloys with trace levels of Sr addition and that the Sr predominantly evolves as the Al_2Si_2Sr phase during the eutectic reaction as normally predicted by fundamental thermodynamics and kinetics. Al_2Si_2Sr phase can be easily enriched at the forefront of the Si phase in the alloy, especially at the root of the branches of eutectic Si phase in Al melt, which leads to constitutional supercooling and prompts a eutectic silicon phase transformation from a lamellar or coarse acicular morphology to fine phase with small particle size. According to MANICKARAJ et al [25] and the results of Fig. 8(e) and Table 4, we can conclude that the modification efficiency of Sr is dependent on the amount, morphology and distribution of Al_2Si_2Sr IMC.

3.3 Effect of Sr or Ti modification on tensile strength of hot-rolled rods of AA4043 welding wire alloy

Figure 9 shows the tensile strength of 9.5 mm AA4043 hot-rolled rods with various contents of Sr or Ti. As can be seen, the tensile strength of the AA4043 hot-rolled rods was improved by adding appropriate amounts of Sr or Ti. These results show that a tensile strength of 97.2 MPa resulted with addition of 0.08% Ti in the Al−5Si alloy, yielding a 11.0% increase above that of the unmodified material, and that the tensile strength decreased slightly with the addition of more Ti to the alloy. When the Sr content in the Al−5Si alloy was 0.025%, the tensile strength of the hot-rolled rod achieved 112 MPa, about 27.9% higher than that of the unmodified rolled alloy rod. These results indicate that Sr addition alone to the alloy resulted in a larger increase in tensile strength than Ti addition alone. Furthermore, the AA4043 hot-rolled rods modified with a combinative addition of 0.025% Sr and 0.08% Ti exhibited the highest tensile strength compared with other hot-rolled rods. The evolution trend of the elongation of the AA4043 hot-rolled rods with adding different contents of Ti and/or Sr was the same as that of the tensile strength of AA4043 hot-rolled rods.

3.4 Effect of Sr or Ti modification on tensile properties and microhardness of AA6082 welds

The effect of varying the Sr or Ti content on the mechanical properties of the 6082 alloy welded joints is shown in Fig. 10. The tensile strength of the base

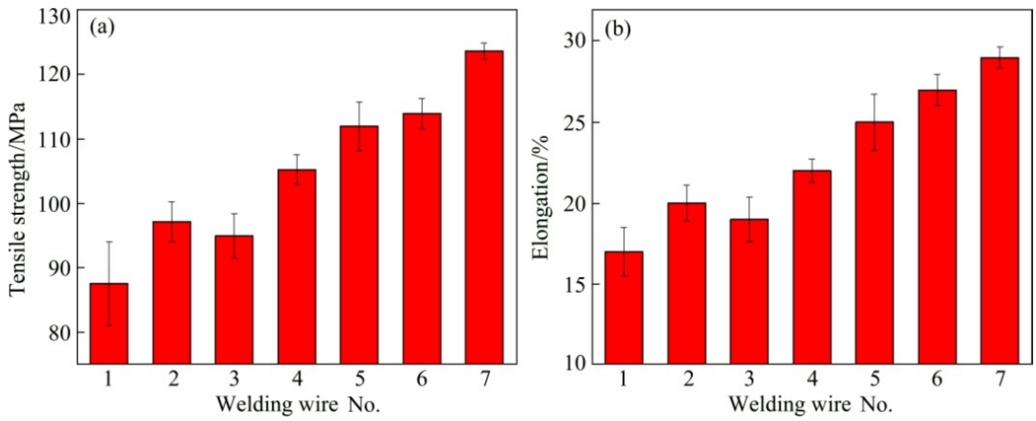

Fig. 9 Effect of Sr or Ti content on tensile strength (a) and elongation (b) of AA4043 hot-rolled rods: 1—0 Ti + 0 Sr; 2—0.08% Ti + 0 Sr; 3—0.15% Ti + 0 Sr; 4—0 Ti + 0.012% Sr; 5—0 Ti + 0.025% Sr; 6—0.08% Ti + 0.012% Sr; 7—0.08% Ti + 0.025% Sr

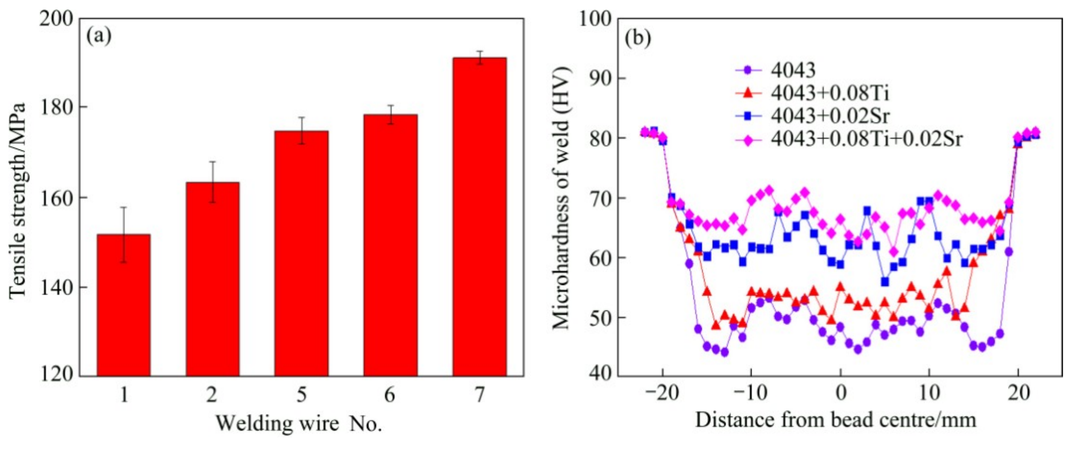

Fig. 10 Tensile properties (a) and transverse microhardness (b) of welds made with different AA4043 welding wires: 1—0 Ti + 0 Sr; 2—0.08% Ti + 0 Sr; 5—0 Ti + 0.025% Sr; 6—0.08% Ti + 0.012% Sr; 7—0.08% Ti + 0.025% Sr

material is 308 MPa. All the tensile data for each condition are an average of measurements made on three specimens. The base metal exhibited high strength compared with TIG welds and was attributed to the Mg_2Si precipitates present in the base metal [26]. As seen from Fig. 10(a), as the alone Ti content was 0.08%, the tensile strength of the butt joints achieved 163.3 MPa, about 7.6% higher than the joints without modification, while the tensile strength of the butt joints reached 174.7 MPa with 0.025% Sr addition alone, which resulted in a 15.2% increase over that of the joints without modification. The tensile strength of the butt joints reached the maximum value when composite Al−5Si−0.08Ti−0.025Sr welding wire was used for TIG welding. Furthermore, as seen from Fig. 9 and Fig. 10(a), the tensile strength standard deviations of hot-rolled rods of composite Al−5Si−0.08Ti−0.025Sr alloy and butt joints welded by Al−5Si−0.08Ti−0.025Sr welding wire is less than those of others.

Transverse microhardness results of the welds are shown in Fig. 10(b). The welds prepared using Al−5Si welding wire modified with 0.08% Ti or 0.02% Sr or using composite Al−5Si−0.08Ti−0.025Sr welding wire exhibited higher hardness compared with unmodified AA4043 welds. This can be attributed to finer grain structure associated with the addition of the modifiers. On the other hand, a hardness reduction in the weld metal and HAZ compared with base metal is evident in all conditions.

Scanning electron images showing the different fracture morphologies of the weld metals are illustrated in Fig. 11. The tensile fracture surfaces of the weld with Ti or Sr modified AA4043 are mostly dimple features, characteristic of a ductile fracture [26]. The finest dimples were observed in AA4043+0.08%Ti+0.025%Sr welds. The massive fine dimples of the tensile fractures and improvement in mechanical properties of welds were attributed to fine microstructures of the weld zone, which resulted from the Ti or Sr modification.

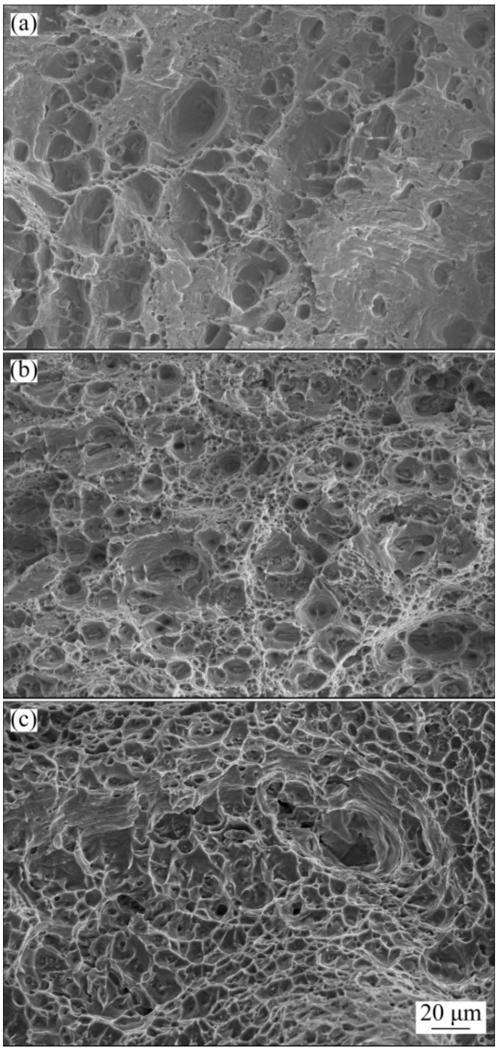

Fig. 11 Tensile fracture surfaces of AA4043 +0.08% Ti weld (a), AA4043 + 0.025% Sr weld (b) and AA4043 + 0.08% Ti + 0.025% Sr weld (c)

4 Conclusions

1) A series of Ti-modified or Sr-modified AA4043 welding wire alloys were developed using a continuous casting and rolling process. The content of Sr was found to progressively decrease with the holding time, while this phenomenon was not observed when Ti was used as the alloy modifier.

2) Addition of 0.08% Ti was found to refine the α(Al) dendrites obviously but was incapable of altering the needle-like morphologies of eutectic Si phases. 0.025% Sr was found to reduce the aspect ratio of needle-like eutectic Si phases significantly but had inadequate capacity of refining α(Al) dendrites. A combinative addition of 0.08% Ti and 0.025% Sr can be mutually complemented in modifying the microstructure of AA4043 welding wire alloy.

3) The mechanical properties of the modified AA4043 hot-rolled rods and the 6082 alloy welded joints using modified AA4043 welding wires were significantly improved. The welds prepared using the AA4043 + 0.08% Ti +0.025% Sr exhibited optimal mechanical properties than AA4043 + 0.08% Ti welds or 4043 + 0.025% Sr welds, which indicated that the combinative addition of Ti and Sr can be an effective composite modifier.

References

[1] EL-LABBAN H F, MAHMOUD E R I. Welding of AA6028 aluminum alloy and its nanocomposite using different filler materials [J]. Materials Transactions, 2015, 56: 113−119.

[2] QIN Guo-liang, SU Yu-hu, WANG Shu-hun. Microstructures and

properties of welded joint of aluminum alloy to galvanized steel by Nd: YAG laser + MIG arc hybrid brazing-fusion welding [J]. Transactions of Nonferrous Metals Society of China, 2014, 24: 989−995.

[3] FADAEIFARD F, MATORI K A, TOOZANDEHJANI M, DAUD A R, ARIFFIN M K A M, OTHMAN N K, GHARAVI F, RAMZANI A H, OSTOVAN F. Influence of rotational speed on mechanical properties of friction stir lap welded 6061-T6 Al alloy [J]. Transactions of Nonferrous Metals Society of China, 2014, 24: 1004−1011.

[4] DAI Wei, XUE Song-bai, LOU Ji-yuan, WANG Shui-qing. Development of Al−Si−Zn−Sr filler metals for brazing 6061 aluminum alloy [J]. Materials & Design, 2012, 42: 395−402.

[5] KUMAR A, SUNDARRAJAN S. Effect of welding parameters on mechanical properties and optimization of pulsed TIG welding of Al−Mg−Si alloy [J]. The International Journal of Advanced Manufacturing Technology, 2009, 42: 118−125.

[6] SEVIM I, HAYAT F, KAYA Y, KAHRAMAN N, ŞAHIN S. The study of MIG weldability of heat-treated aluminum alloys [J]. The International Journal of Advanced Manufacturing Technology, 2013, 66: 1825−1834.

[7] AHMAD R, BAKAR M A. Effect of a post-weld heat treatment on the mechanical and microstructure properties of AA6061 joints welded by the gas metal arc welding cold metal transfer method [J]. Materials & Design, 2011, 32: 5120−5126.

[8] VERMA R P, PANDEY K N, SHARMA Y. Effect of ER4043 and ER5356 filler wire on mechanical properties and microstructure of dissimilar aluminium alloys, 5083-O and 6061-T6 joint, welded by the metal inert gas welding [J]. Proceedings of the Institution of Mechanical Engineers, Part B: Journal of Engineering Manufacture, 2015, 229: 1021−1028.

[9] RAMANAIAH N, RAO K S, GUHA B, RAO K P. Effect of modified AA4043 filler on partially melted zone cracking of Al-alloy gas tungsten arc welds [J]. Science and Technology of Welding & Joining, 2005, 10: 591−596.

[10] BABU N K, TALARI M K, DAYOU P, ZHENGA S, JUNA W, SIVAPRASADC K. Influence of titanium–boron additions on grain refinement of AA6082 gas tungsten arc welds [J]. Materials & Design, 2012, 40: 467−475.

[11] HU Zhi, RUAN Xian-ming, YAN Hong. Effects of neodymium addition on microstructure and mechanical properties of near-eutectic Al−12Si alloys [J]. Transactions of Nonferrous Metals Society of China, 2015, 25: 3877−3885.

[12] LI J H, BARRIRERO J, ENGSTLER M, ABOULFADL H, MÜCKLICH F, SCHUMACHER P. Nucleation and growth of eutectic Si in Al−Si alloys with Na addition [J]. Metallurgical and Materials Transactions A, 2015, 46: 1300−1311.

[13] BABU N K, TALARI M K, DAYOU P, ZHENG Sun, JUN Wei, SivaPrasad K. Influence of titanium–boron additions on grain refinement of AA6082 gas tungsten arc welds [J]. Materials & Design, 2012, 40: 467−475.

[14] TSAI Y C, CHOU C Y, LEE S L, LIN C K, LIN J C, LIM S W. Effect of trace La addition on the microstructures and mechanical properties of A356 (Al−7Si−0.35 Mg) aluminum alloys [J]. Journal of Alloys and Compounds, 2009, 487: 157−162.

[15] ONYIA C W, OKORIE B A, NEIFE S I, OBAYI C S. Structural modification of sand cast eutectic Al−Si alloys with sulfur/sodium and its effect on mechanical properties [J]. World Journal of Engineering and Technology, 2013, 1: 9−16.

[16] JIANG Wen-ming, FAN Zi-tian, DAI Yu-cheng, LI Chi. Effects of rare earth elements addition on microstructures, tensile properties and fractography of A357 alloy [J]. Materials Science and Engineering A, 2014, 597: 237−244.

[17] BIROL Y. Effect of silicon content in grain refining hypoeutectic Al−Si foundry alloys with boron and titanium additions [J]. Materials Science and Technology, 2012, 28: 385−389.

[18] LIAO Heng-cheng, SUN Guo-xiong. Mutual poisoning effect between Sr and B in Al−Si casting alloys [J]. Scripta Materialia, 2003, 48: 1035−1039.

[19] GUSIEVA K, DAVIES C H J, SCULLY J R, BIRBILIS N. Corrosion of magnesium alloys: The role of alloying [J]. International Materials Reviews, 2015, 60: 169−194.

[20] SHABESTARI S G, MIRESMAEILI S M, BOUTORABI S M A. Effects of Sr-modification and melt cleanliness on melt hydrogen absorption of 319 aluminium alloy [J]. Journal of Materials Science, 2003, 38: 1901−1907.

[21] LIU L, SAMUEL A M, SAMUEL F H, DOTY H W, VALTIERRA S. Influence of oxides on porosity formation in Sr-treated Al−Si casting alloys [J]. Journal of Materials Science, 2003, 38: 1255−1267.

[22] ZEREN M, KARAKULAK E. Influence of Ti addition on the microstructure and hardness properties of near-eutectic Al−Si alloys [J]. Journal of Alloys and Compounds, 2008, 450: 255−259.

[23] YANG Jin-long, XUE Song-bai, DAI Wei, XUE Peng. Saturation phenomenon of Ce and Ti in the modification of Al−Zn−Si filler metal [J]. International Journal of Minerals, Metallurgy, and Materials, 2015, 22: 184−189.

[24] HAMILTON D R, SEIDENSTICKER R G. Growth mechanisms of germanium dendrites: Kinetics and the nonisothermal interface [J]. Journal of Applied Physics, 1963, 34: 1450−1460.

[25] MANICKARAJ J, GORNY A, CAI Zhong-hou, SHANKAR S. X-ray nano-diffraction study of Sr intermetallic phase during solidification of Al−Si hypoeutectic alloy [J]. Applied Physics Letters, 2014, 104: 073102.

[26] MISSORI S, SILI A. Mechanical behaviour of 6082-T6 aluminium alloy welds [J]. Metallurgical Science and Technology, 2000, 18: 12−18.

复合添加 Ti 和 Sr 对 AA4043 铝合金焊丝变质和 AA6082 TIG 焊接接头力学性能的影响

王 博[1]，薛松柏[1]，马超力[1]，韩翼龙[1]，林中强[2]

1. 南京航空航天大学 材料科学与技术学院，南京 210016；2. 浙江宇光铝材有限公司，金华 321200

摘　要：为提高采用 AA4043 焊丝焊接的 AA6082 钨极氩弧焊接头的力学性能，研究了元素 Ti 和 Sr 对连铸连轧 AA4043 焊丝的影响。结果表明：元素 Ti、Sr 变质效果较好，可以改善 AA4043 焊丝的显微组织，并提高 AA6082 焊缝的力学性能。与单独添加元素 Ti 或 Sr 相比，复合添加两种元素可以同时高效地变质 α(Al)枝晶和共晶 Si 相。此外，元素 Ti、Sr 可以改善 AA6082 焊缝的显微组织，当复合添加 0.08% Ti 和 0.025% Sr 时，AA6082 焊缝的抗拉强度达到最大。结果表明，Ti 和 Sr 的复合添加可以实现较好的变质效果。

关键词：AA4043 焊丝；钛；锶；变质；钨极氩弧焊；显微组织；力学性能

(Edited by Xiang-qun LI)